ACS APPLIED MATERIALS & INTERFACES

Research Article

www.acsami.org

Bioreducible Polymer Nanocarrier Based on Multivalent Choline Phosphate for Enhanced Cellular Uptake and Intracellular Delivery of Doxorubicin

Wenliang Wang,[†,‡] Bo Wang,[†] Sanrong Liu,[†] Xudong Shang,[†] XinXin Yan,[†,‡] Zonghua Liu,[§] Xiaojing Ma,*[,†] and Xifei Yu*[,†,‡]

[†]The Polymer Composites Engineering Laboratory, Changchun Institute of Applied Chemistry, Chinese Academy of Sciences, Changchun 130022, P.R. China

[‡]University of Science and Technology of China, Hefei 230026, P.R. China.

[§]Department of Biomedical Engineering, Jinan University, Guangzhou 510632, P.R. China

Supporting Information

ABSTRACT: Limited cellular uptake and inefficient intracellular drug release severely hamper the landscape of polymer drug nanocarriers in cancer chemotherapy. Herein, to address these urgent challenges in tumor treatment simultaneously, we integrated the multivalent choline phosphate (CP) and bioreducible linker into a single polymer chain, designed and synthesized a neoteric bioreducible polymer nanocarrier. The excellent hydrophility of these zwitterionic CP groups endowed high drug loading content and drug loading efficiency of doxorubicin to this drug delivery system (~22.1 wt %, ~95.9%). Meanwhile, we found that the multivalent choline phosphate can effectively enhance the internalization efficiency of this drug-loaded nanocarrier over few seconds, and the degree of improvement depended on the CP density in a single polymer chain. In addition, after these nanocarriers entered into the tumor cells, the accelerated cleavage of bioreducible linker made it possible for more cargo escape from the delivery system to cytoplasm to exert their cytostatic effects more efficiently. The enhanced therapeutic efficacy in various cell lines indicated the great potential of this system in anticancer drug delivery applications.

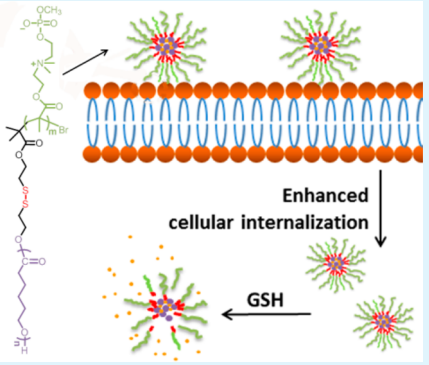

KEYWORDS: *choline phosphate, polymer nanocarriers, bioreducible linker, cellular internalization, cancer therapy*

1. INTRODUCTION

Polymer drug nanocarriers have received tremendous attention as an emerging tool for cancer chemotherapy because of their characteristic properties that increase drug bioavailability, prolong circulation time, circumvent the drug efflux pumps, and promote accumulation in the tumor via enhanced permeability and retention (EPR) effect.[1−3] For example, the biomimetic phosphorylcholine (PC)-based copolymers have been exploited to deliver doxorubicin (Dox) and shown remarkable bioavailability and minimized cardiotoxicity.[3−6] In addition, the biodegradable poly(ε-caprolactone) has also been extensively integrated into the delivery system as the core of nanocarriers to load hydrophobic anticancer drug via van der Waals force.[7−10] However, the sluggish cellular internalization as well as the inefficient intracellular drug release of these polymer drug loaded nanocarriers severely results in the intracellular concentration of anticancer drugs below the required therapeutic level and the inefficient chemotherapy efficacy,[11] which greatly limited its application in practical therapy. To address the challenges, a few strategies have been proposed: (i) utilization of cationic domains, such as polyethylenimine to enhance the attraction between the nanocarriers and the anionic cell surface;[12−17] (ii) optimizing the shape of the nanocarriers, for example, tubular and long cylindrical morphology to improve circulation time and cell internalization;[18−22] (iii) natural ligands (e.g., folic acid, RGD) have also been introduced to facilitate cellular uptake by targeting nanocarriers to specific receptors out of the cell surface;[23−25] (iv) decorating with boronic acid to improve the cellular internalization via diol-boronate ester formation with cell surface glycoproteins.[26−28]

Although great progress have been achieved, it is still desirable to develop new neoteric tactics to better solve these challenges, especially those that can both enhance cellular internalization and intracellular drug release at the same time. Inspired from the phosphatidylcholine groups (PC, the headgroup of phospholipids existed in mammalian cells and at least 10% of all bacterial), Yu et al. first synthesized the "PC-

Received: March 8, 2017
Accepted: April 5, 2017
Published: May 8, 2017

DOI: 10.1021/acsami.7b03317
ACS Appl. Mater. Interfaces 2017, 9, 15986−15994

reverse" choline phosphate (CP), and confirmed that the choline phosphate in a multivalent fashion can rapidly and reversibly bind to various cell membranes and to PC-containing liposomes.[29−34] Meanwhile, we prepared a neoteric prodrug system decorated with multivalent CP groups, which shown enhanced cellular internalization and improved cancer therapy efficacy.[35] In addition, other studies also showed that CP groups are compatible with human physiology, appearing in tissue engineering, localized drug delivery and other remedies.[36−38] On the basis of the recent studies in choline phosphate, we propose a novel perspective to overcome the inefficient cellular internalization and intracellular drug release for these drug loaded polymer nanocarriers simultaneously.

Here we prepared the polymer nanocarrier constructed with poly(choline phosphate) and poly(ε-caprolactone) (PCL), which were linked by disulfide bond, then furtherly demonstrated that the use of multivalent choline phosphate was conducive to enhance the delivery of Dox into the cancer cells (as shown in Scheme 1), and the degree of improvement

Scheme 1. Schematic Illustration of Cellular Internalization and Its Intracellular Drug Release of the Dox-Loaded PMCP-s-s-PCL Nanoparticles

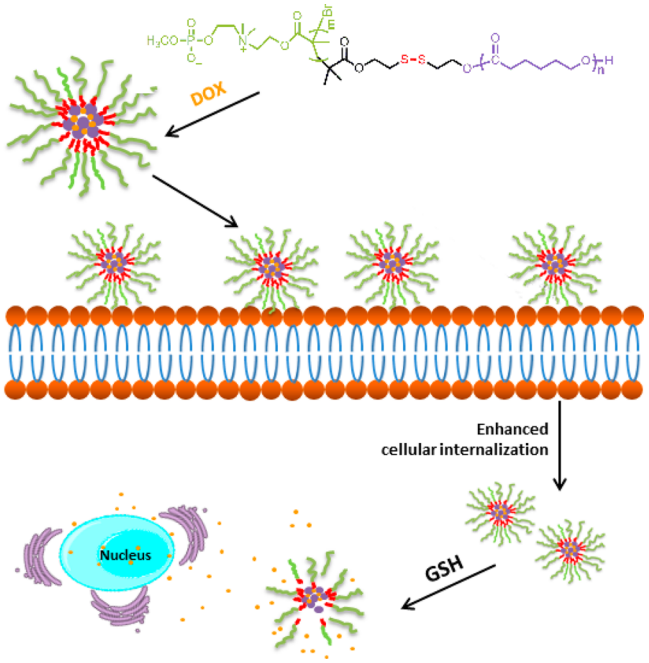

depended on the CP density in a single polymer chain. On the other hand, the excellent hydrophility of these zwitterionic CP groups endowed high drug loading content and drug loading efficiency of Dox to this drug delivery system (~22.1 wt %, ~95.9%). In addition, it has been found that the concentration of glutathione (GSH) in intracellular compartments is as high as 2−10 mM, although it becomes much smaller than that in extracellular milieu (<10 μM).[39−43] Considering the large redox potential difference between extra- and intracellular compartments, the redox-cleavable disulfide bonds were introduced to improve intracellular drug release in response to intracellular levels of glutathione. The cell viability assay demonstrated that the Dox-loaded polymer nanocarriers we reported here exhibited enhanced efficacy of cancer chemotherapy in different tumor cell lines. It provided novel perspective for addressing these therapeutic challenges of tumors by using polymer drug nanocarrier, which are currently considered difficult to overcome.

2.1. Materials. The synthesis of 2-(methacryloyloxy) ethyl choline phosphate (MCP) has been reported by previous methods.[29,35] 2-hydroxyethyl disulfide (technical grade,) doxorubicin hydrochloride (Dox·HCl), copper(I) bromide (CuBr, 99.999%), 2-methacryloyloxyethyl phosphorylcholine (MPC), tin(II) 2-ethylhexanoate ($Sn(Oct)_2$), and 2,2-bipyridine (bpy) were purchased from Sigma-Aldrich. Triethylene glycol, α-bromoisobutyryl bromide (Br-iBuBr) and ε-caprolactone were purchased from J&K Chemical. The ε-caprolactone monomer was dried over CaH_2 for 24 h and distilled under vacuum before use. Toluene was dried through refluxing over Na and distilled before use. The MPC monomer was washed with THF three times to remove the polymerization inhibitor before use. All chemicals were used without further purification unless otherwise mentioned.

2.2. Characterization. The ^1H and ^{31}P NMR spectra were recorded on the Unity-400 NMR spectrometer using DMSO-d_6, CD_3OD, or $CDCl_3$ as the solvent. The size distribution of these copolymer delivery systems in aqueous medium was measured via DLS on Zetasizer Nano-ZS. In addition, the morphology of these nanoparticles was measured by transmission electron microscopy (TEM) using JEOL JEM-1011 electron microscope. The molecular weight and polydispersity of the polymers PCL-Br and PCL-s-s-Br were determined by gel permeation chromatography (GPC, Waters 1525). THF was used as eluent solution and polystyrene as standard. Meanwhile, the UV−vis spectroscopy (NnanoDrop 2000c) was used to determine the Dox content accommodated in the nanoparticles. The fluorescent intensity of Dox internalized into the cells was recorded via confocal laser scanning microscopy (LSM 700 Carl Zeiss Microscopy) and flow cytometry (FACS, Guava easyCyte 6−2L from Milipore). What's more, the synergy microplate reader (Synergy H1, from Bio Tek) was used to detect the call viability.

2.3. Synthesis of 2-[(2-hydroxyethyl)disulfanyl]ethyl 2-bromo-2-methylpropanoate (HO-s-s-Br). The synthesis of HO-s-s-Br was according to previous methods.[8,44] 2-Hydroxyethyl disulfide (3.1 g, 0.02 mol) and trimethylamine (2.53 g, 0.025 mol) were dissolved in dichloromethane (CH_2Cl_2, 50 mL). Br-iBuBr (2.3 g, 0.01 mol) dissolved in 15 mL CH_2Cl_2 was added dropwise at 0 °C over 30 min to above mixed solution. The resulting mixture was stirred for 24 h at room temperature and the white solids were removed by vacuum filtration. The filtrate was washed with water three times, and dried with anhydrous $MgSO_4$. The CH_2Cl_2 was removed by rotary evaporation and the residue was purified by silica column chromatography with a mixture of CH_2Cl_2/ ethyl acetate (5/1, v/v). The product was collected by removing the solution with yield 33%. ^1H NMR (400 MHz, $CDCl_3$): Figure 1a, δ (ppm) 4.45 (t, -C***H***$_2$OC(O)−), 3.89 (t, -C***H***$_2$−OH), 2.97 (t, -s-s-C***H***$_2$-CH$_2$OC(O)−), 2.89 (t, HO−CH$_2$−C***H***$_2$-s-s-), 1.94 (s, -C(C***H***$_3$)$_2$Br).

2.4. Synthesis of PCL-s-s-Br. The PCL-s-s-Br was synthesized via ring-opening polymerization (ROP) under the catalysis of $Sn(Oct)_2$. Simply, HO-s-s-Br (0.182 g, 0.6 mmol), ε-caprolactone (4.78 g, 42 mmol) and $Sn(Oct)_2$ (0.122 g, 0.3 mmol) were added to a dry flask containing 15 mL anhydrous toluene, where the flask was flame-dried and protected by argon before using. Then, the resulting solution was degassed through three exhausting/refilling argon cycles, and the reaction was carried out for 5 h at 110 °C with continuous stirring. The

DOI: 10.1021/acsami.7b03317
ACS Appl. Mater. Interfaces 2017, 9, 15986−15994

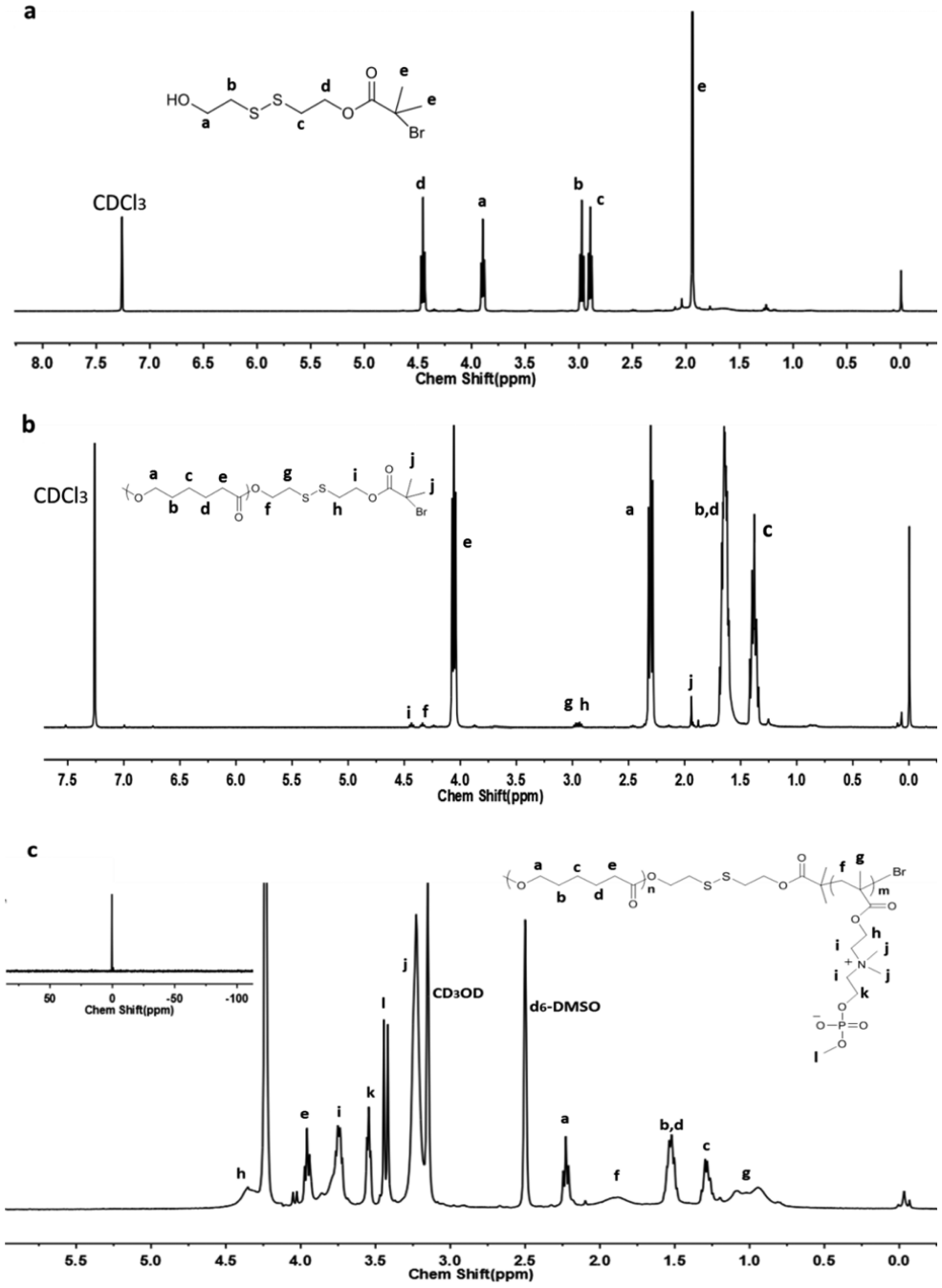

Figure 1. (a) ^{1}H NMR spectra of HO-s-s-Br, (b) ^{1}H NMR spectrum of PCL-s-s-Br, (c) ^{1}H NMR, and ^{31}P NMR spectra of PMCP-s-s-PCL.

mixture was concentrated and precipitated third times in cold diethyl ether. Finally, the precipitate was collected and dried under vacuum at 30 °C for 24 h with yield 82.4%. ^{1}H NMR (400 MHz, CDCl3): Figure 1b, 4.06 (t, -C***H***$_2$COO−), 2.30 (t,−O-C***H***$_2$-CH$_2$−), 1.64 (m, -OCH$_2$−C***H***$_2$-CH$_2$−C***H***$_2$-CH$_2$−COO−), 1.38 (m, -OCH$_2$−CH$_2$−C***H***$_2$-CH$_2$−CH$_2$−COO−).

2.5. Synthesis of PCL$_{90}$-s-s-PMCP. The typical ATRP procedure consulted previous methods.[30,35] PCL$_{90}$-s-s-Br (0.528 g, 0.05 mmol), MCP (1.475g, 5 mmol), bpy (31.2 mg, 0.2 mmol) and solvent (mixture of 4 mL THF and 3 mL methanol) were added to a Schlenk flask. The mixture was degassed by three exhausting/refilling dry nitrogen cycles, and then the CuBr (14.3 mg, 0.1 mmol) was added under the nitrogen. The polymerization was carried out at room temperature for 36 h, and then quenched by exposing the mixture to air. Finally, the solution was diluted by water, and then put into the dialysis bag with MCWO-3500 to dialyze for 24 h to remove the excessive catalyst and monomer. After lyophilized, the PCL$_{90}$-s-s-PMCP was collected (yield 71.9%). ^{1}H NMR (400 MHz, d_6-DMSO and CD$_3$OD): Figure 1c, δ (ppm) 4.35 (s, -C***H***$_2$O−CO−), 3.96 (t, -C***H***$_2$COO−), 3.75 (m, -C***H***$_2$N(CH$_3$)$_2$-C***H***$_2$-), 3.55 (t, -POC***H***$_2$-), 3.44−3.42 (d, -POC***H***$_3$), 3.23 (s, -N-(C***H***$_3$)$_2$), 2.23 (t,−O-C***H***$_2$-CH$_2$−), 1.88 (s, −CC***H***$_2$C−), 1.54 (m, -OCH2-C***H***$_2$-CH2-C***H***$_2$-CH$_2$−COO−), 1.28 (m, -OCH2-CH$_2$−C***H***$_2$-CH$_2$−CH$_2$−COO−), 1.09−0.93 (d, −CC***H***$_3$); ^{31}P NMR (400 MHz, d_6-DMSO and CD$_3$OD): δ(ppm) 0.96 (s).

DOI: 10.1021/acsami.7b03317
ACS Appl. Mater. Interfaces 2017, 9, 15986−15994

Scheme 2. Synthetic Strategies for the Polymer of PMCP-s-s-PCL, and the Chemical Structure for Control of Both PCL-s-s-PMPC and PCL-b-PMCP

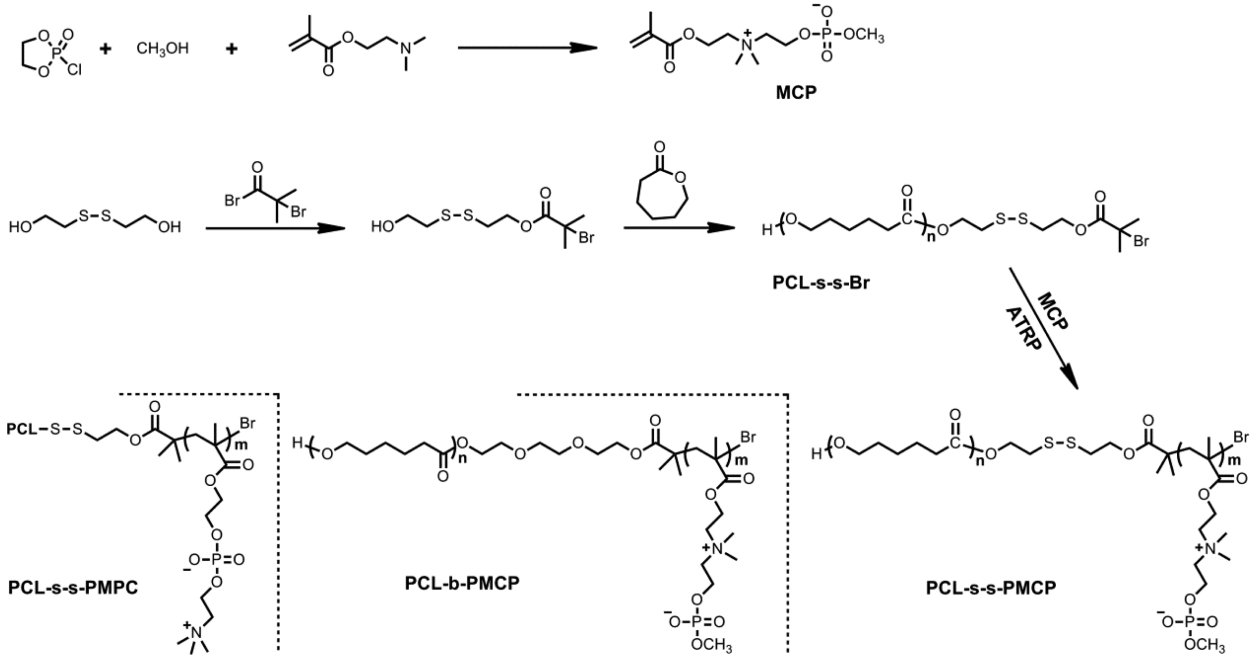

2.6. Preparation of Blank and Drug-Loaded Nanoparticles. The diblock copolymers (30 mg) of PMCP-s-s-PCL, PMPC-s-s-PCL or PMCP-*b*-PCL were dissolved in 1 mL mixed solution (methanol: DMSO, 1:1, v/v) respectively, and stirred at room temperature for 1 h. Then, the mixture was added dropwise to 20 mL of deionized water with continue stirring. After stirred for another 4 h, the solution was dialyzed against 1 L deionized water for 24 h (MWCO 3500) to remove the solvent, and the deionized water was exchanged every 6 h. The size and polydispersity were determined by DLS.

2.7. Preparation of Dox-Loaded Nanoparticles. Following the blank nanoparticles preparation method described above. The diblock copolymers (30 mg) of PMCP-s-s-PCL, PMPC-s-s-PCL, PMCP-*b*-PCL, respectively, and 9 mg Dox·HCl were dissolved in 1 mL mixed solution (methanol: DMSO, 1:1, v/v), and then trimethylamine (10 μL) was added to the mixture to remove the HCl of Dox·HCl, and then the solution was stirred at room temperature for 1 h. Subsequently, the mixture was added dropwise to 20 mL deionized water with continue stirring. After stirred for another 4 h, the solution was dialyzed against 1 L of deionized water for 24 h (MWCO 3500) to remove the solvent, and the deionized water was exchanged every 6 h. To determine the total loading of Dox, we lyophilized the dialysate, and redispersed Dox-loaded nanoparticle (1 mg) in deionized water. The UV absorbance at 488 nm was measured to determine the total loading of Dox. Drug loading content (DLC) and drug loading efficiency (DLE) were calculated according to the eqs 1 and 2.

$$\mathrm{DLC}(\%) = \frac{\text{weight of drug encapsulated in nanoparticles}}{\text{weight of polymer}} \times 100\% \quad (1)$$

$$\mathrm{DLE}(\%) = \frac{\text{weight of drug encapsulated in nanoparticles}}{\text{weight of drug in feed}} \times 100\% \quad (2)$$

2.8. In Vitro Drug Release. The release of Dox from drug-loaded PMCP-s-s-PCL and PMPC-*b*-PCL nanoparticles was examined using a dialysis method against phosphate buffered saline (PBS) with or without 10 mM glutathione at 37 °C. Drug-loaded nanoparticles (3 mg) redispersed in PBS (2 mL, with or without 10 mM glutathione) were dialyzed against PBS (18 mL, with or without 10 mM glutathione) with constant stirring at 37 °C. At fixed time intervals, the outside buffer solution (1 mL) was taken out to determine the concentration of Dox via UV−vis measurements respectively, and replenished with an equal volume of fresh medium. The total release amount of Dox was determined by the previous method.[35]

2.9. Cellular Uptake Assays. *Flow cytometry.* MCF-7, A549 and HePG-2 cells were grown in Dulbecco's modified Eagle's medium (DMEM) with high glucose containing 10% fetal bovine serum (FBS), streptomycin (100 μg/mL) and 100 units per mL of penicillin at 37 °C, respectively. Then cells were transferred to 12-well plates with the density of 2×10^5 cells per well and incubated for 1 day. Afterward, the medium was removed and the fresh serum-free DMEM including free Dox, Dox loaded nanoparticles (PMCP-s-s-PCL, PMPC-s-s-PCL, PMCP-*b*-PCL) were added, respectively. The concentration of Dox in all medium was 10 μg/mL. After incubated for fixed time, the medium was removed, and the plates were washed with PBS. The cells were digested with trypsin and collected after centrifugation. Finally, the cells were resuspended in 0.3 mL of PBS to determine the internalization efficiency with flow cytometer.

Confocal Laser Scanning Microscopy. MCF-7, A549, and HePG-2 cells were grown in Dulbecco's modified Eagle's medium (DMEM) with high glucose containing 10% fetal bovine serum (FBS), streptomycin (100 μg/mL) and 100 units per mL of penicillin at 37 °C. The cells were then transferred to 12-well plates with the density of 2×10^5 cells per well and incubated for 1 day. Afterward, the medium was removed and the fresh serum-free DMEM including free Dox, Dox-loaded $PMCP_{120}$-s-s-PCL_{90}, and $PMPC_{150}$-s-s-PCL_{90} were added,

DOI: 10.1021/acsami.7b03317
ACS Appl. Mater. Interfaces 2017, 9, 15986−15994

respectively. After incubation at 37 °C for corresponding time intervals, the medium was removed, and the plates were washed with PBS. Then, 4% formaldehyde was added to fix the cell for 30 min at room temperature. Th cell nuclei were then stained with 4′,6-diamidino-2-phenylindole (DAPI, 10 μg/mL) for 10 min and washed at least four times with cold PBS. Finally, the CLSM images were taken using confocal microscope.

Cell Viability Assay. MCF-7, A549 and HePG-2 cells were transferred to 96-well flat-bottomed plates with density of 9 × 10^3 cells per well and incubated for 1 day. Afterward, the medium was removed and the fresh serum-free DMEM including free Dox, Dox-loaded $PMCP_{120}$-s-s-PCL_{90}, $PMPC_{150}$-s-s-PCL_{90} and $PMCP_{83}$-*b*-PCL_{77} were added, respectively. After incubated for 2 h, the medium was removed, and the plates were washed twice times with cold PBS, then the fresh serum-free DMEM was added. After incubated for another 22 h, 10 μL of Celltiter-Blue reagent was added to each well and the cells were incubated for another 4 h. The cell viability was detected via microplate reader (λ_{ex} = 560 nm, λ_{em} = 590 nm). The cell viability was calculated based on the eq 3.

$$\text{cell viability}(\%) = \frac{\text{fluorescent intensity(sample)}}{\text{fluorescent intensity(control)}} \times 100\% \quad (3)$$

3. RESULTS AND DISCUSSION

3.1. Synthesis of the Polymer Drug Delivery System PMCP-s-s-PCL. The synthetic method of diblock copolymer PMCP-s-s-PCL was shown in Scheme 2. First, the dual initiator HO-s-s-Br with a disulfide and terminal groups of OH and Br was synthesized via a simple condensation reaction in the presence of 2-hydroxyethyl disulfide and Br-iBuBr, and the ^{1}H NMR (Figure 1a) demonstrated the high purity of this product. Then, the PCL-s-s-Br was prepared by ring-opening polymerization under the catalysis of $Sn(Oct)_2$ in toluene at 110 °C, where the polymerization degree of these polymers could be well controlled by adjusting the mole ratio of HO-s-s-Br and ε-caprolactone monomer. The M_n of these macroinitiators was determined from the ^{1}H NMR (Figure 1b) through comparison of the integrals of HO-s-s-Br (δ 1.94) and PCL (δ 4.06, δ 2.30, δ 1.64, δ 1.38), and the GPC data (Table 1 and Figure S3) indicated these polymers had a low polydispersity.

Subsequently, with the aid of the ATRP, the diblock copolymer PMCP-s-s-PCL with various polymerization degree were obtained using the PCL-s-s-Br as macroinitiator (^{1}H NMR and ^{31}P NMR spectrum were shown in Figure 1c), and the M_n was calculated from the ^{1}H NMR through comparison of the integrals of HO-s-s-Br (δ 1.94), PCL (δ 4.06, δ 2.30, δ 1.64, δ 1.38) and PMCP (δ 3.75, δ 3.55, δ 3.44, δ 3.23). In addition, we also synthesized the series of diblock copolymer PMPC-s-s-PCL and PMPC-*b*-PCL as control (^{1}H NMR spectrum was shown in Figures S2a–d), the detailed synthesis procedure are shown in Scheme S1.

Table 1. Molecular Weight and Polydispersities of Polymers

entries	polymers	M_n[a] g·mol^{-1}	M_n[b] g·mol^{-1}	PDI[a]	PMCP mol %
1	PCL_{77}-Br	14247	9077	1.45	n/a
2	PCL_{90}-s-s-Br	11431	10559	1.25	n/a
3	PCL_{120}-s-s-Br	15856	13979	1.50	n/a
4	$PMCP_{85}$-*b*-PCL_{77}	n/a	34152	n/a	52%
5	$PMCP_{120}$-s-s-PCL_{90}	n/a	45660	n/a	57%
6	$PMPC_{150}$-s-s-PCL_{90}	n/a	54809	n/a	63%(PC)

[a]Measured by GPC (THF as eluent, PS as standards). [b]Calculated by the ^{1}HMR spectrum.

3.2. Preparation and Characterization of Nanoparticles. After dissolved in mixed solution (DMSO: CH_3OH, 1:1, v/v) and dialyzed against water, PMCP-s-s-PCL were able to self-assemble into nanoparticles driven by the hydrophobic PCL core as well as hydrophilic PMCP outer shell. As shown in Figure 2 and Table 2, the TEM and DLS measurements

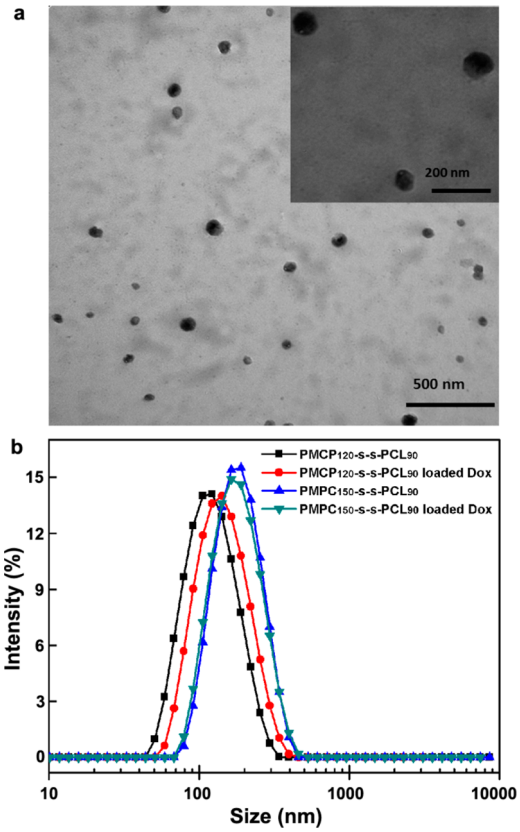

Figure 2. (a) TEM image of $PMCP_{120}$-s-s-PCL_{90} nanoparticles, (b) the size distribution of $PMCP_{120}$-s-s-PCL_{90} and $PMPC_{150}$-s-s-PCL_{90} nanoparticles before and after loading Dox in aqueous solution.

indicated that these nanoparticles had a desirable size range (<200 nm) and a narrow polydispersity (<0.290), which effectively circumvented the uptake of reticuloendothelial system, minimized the renal excretion and enhanced the EPR effect for passive tumor targeting.[45] In addition, it can be found that after loading the drug the size of nanoparticles became larger, which maybe because that the hydrophobic Dox was accommodated into the nanoparticle via van der Waals interaction, which expanded the core of the nanoparticles and rendered the size increase.

In general, because the relatively low DLC and DLE of traditional drug delivery systems, the high dosage of polymer carrier was required to increase the anticancer drug concentration in cells up to the therapeutic level, which inevitably generated new concerns, such as the degradation, and biological toxicity of these carriers.[46,47] Impressively, the PMCP-s-s-PCL we synthesized here showed tremendous

DOI: 10.1021/acsami.7b03317
ACS Appl. Mater. Interfaces 2017, 9, 15986–15994

Table 2. Hydrodynamic Size and PDI of Polymer Nanoparticles Determined by DLS

entries	polymers	size[a] (nm)	PDI[a]	size[b] (nm)	PDI[b]	DLC (%)	DLE (%)
1	$PMCP_{85}$-*b*-PCL_{77}	129.6	0.285	147.3	0.288	18.41	79.80
2	$PMCP_{50}$-s-s-PCL_{90}	115.0	0.113	precipitate	n/a	n/a	n/a
3	$PMCP_{90}$-s-s-PCL_{90}	125.4	0.204	132.6	0.199	21.37	92.61
4	$PMCP_{110}$-s-s-PCL_{90}	110.7	0.178	135.5	0.164	18.59	80.56
5	$PMCP_{120}$-s-s-PCL_{90}	113.6	0.146	138.8	0.225	22.13	95.91
6	$PMCP_{180}$-s-s-PCL_{90}	191.6	0.174	266.4	0.123	19.82	85.9
7	$PMPC_{150}$-s-s-PCL_{90}	155.6	0.137	164.3	0.380	14.44	62.65

[a]Before loading Dox. [b]After loading Dox.

potential to improve the DLC and DLE of the drug delivery system. According to the data in Table 2, the DLC and DLE of this delivery system can be calculated to as high as to be 22.1 wt % and 95.9%, respectively, which was much larger than the reported delivery systems (<10 wt %).[45,48,49] The enhanced loading capacity was attributed to the excellent hydrophility of PMCP shell, which stabilized the nanoparticle in case it precipitated at high loading content.

3.3. Enhanced Cellular Internalization. As a proof of concept, we determined whether the delivery system with multivalent CP groups can largely enhance the cellular internalization over a short time. At first, we qualitatively measured the internalization efficiency of Dox using CLSM, where the red fluorescence intensity was corresponding to the internalization efficiency of Dox. It can be seen from Figure 3

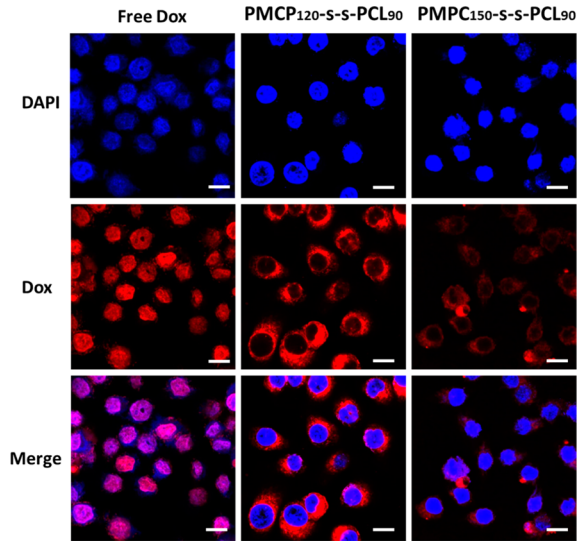

Figure 3. Confocal images of MCF-7 cells incubated 1 h by free Dox (10 μg/mL), Dox-loaded polymers (Dox equivalent concentration: 10 μg/mL) of $PMCP_{120}$-s-s-PCL_{90}, $PMCP_{85}$-*b*-PCL_{77}, and $PMPC_{150}$-s-s-PCL_{90} (as control). Scale bar: 20 μm.

that after MCF-7 cells was incubated with various Dox-loaded nanoparticles and free Dox for 1 h, the nanoparticles decorated with multivalent CP exhibited higher red fluorescence intensity than the these without CP, confirmed that the integration of multivalent CP into delivery systems can significantly enhance the cellular internalization. Because the nanoparticles sizes are in the same range (100−200 nm) and the polydispersity is narrow (Table 2), the enhanced cellular internalization should be caused by the strong interactions of polyvalent CP and PC-lipids in cell membrane instead of the diverse size effect. Meanwhile, we observed the same results in another two tumor cell lines A549 and HePG-2, as shown in Figures S4 and S5, which means that the enhanced internalization efficiency caused by the addition of CP is universal in various tumor cell lines.

Subsequently, to further confirm that the multivalent CP can indeed enhance the cellular internalization, and to discuss the influence of CP density to cellular internalization efficiency, we further detected the fluorescence intensity of MCF-7 cells incubated with free Dox, various Dox-loaded PMCP-s-s-PCL, PMCP-*b*-PCL, and PMPC-s-s-PCL for fixed time intervals (0.5h, 1h, 2h) using flow cytometry. As shown in Figure 4

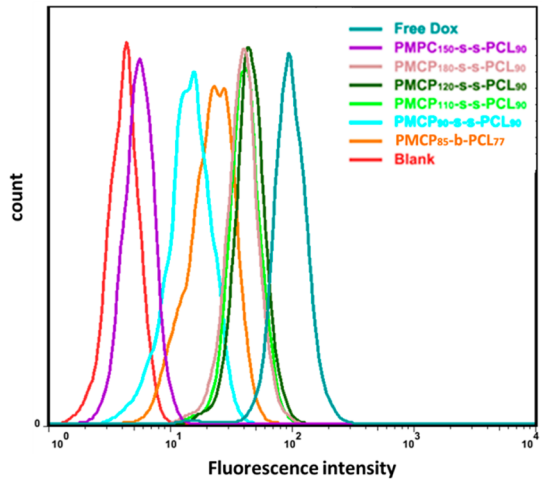

Figure 4. Overlays of flow cytometry of MCF-7 cells incubated 1 h by Dox (10 μg/mL), series of polymers (Dox equivalent concentration: 10 μg/mL) of Dox-loaded PMCP-s-s-PCL, and Dox-loaded PMPC-s-s-PCL (as control).

Figure S6, although the internalization efficiency of all these kind of nanoparticles was enhanced with the prolong of incubation time, the Dox-loaded nanoparticles with multivalent CP were much more efficiently uptake at fixed time intervals, and the fluorescence signal incubated by the nanoparticle without CP groups was weak, indicating the sluggish and inefficient internalization for this kind of nanoparticle. In addition, considering the existence of serum in the practical application, we investigated the cellular internalization of this CP-based nanocarrier in the presence of serum by using flow cytometry (as shown in Figure S7), and also compared the results in the absence and presence of serum. It was found that in this CP decorated nanocarriers the serum has no obvious influence on its cellular internalization. What's more, the internalization efficiency enhanced as the increase of CP density, but the tendency became smaller after the polymerization degree of MCP was up to 120. We applied the same experiments on another two tumor cell lines, A549 and HePG-

DOI: 10.1021/acsami.7b03317
ACS Appl. Mater. Interfaces 2017, 9, 15986−15994

2 (Figures S8 and S9), and showed same tendency on their cellular internalization. The FACS results were consistent well with the previous CLSM results, which further indicated the delivery systems with multivalent CP may be internalized by tumor cells with faster speed and higher efficiency over few second.

Different from the passive diffusion of small-molecule drugs, the polymer nanocarriers entered into the cells mainly by active or passive endocytosis,[46,50−53] which has been proven to be inefficient since it is a sluggish process for polymer nanocarriers to bind to the cell membranes. In our experiment, multivalent CP were successfully introduced to the polymer and existed as out shell in the formed nanoparticles due to is strong hydrophilicity. The specific and strong interaction between multivalent CP and membranes accelerated these delivery systems to bind to the tumor cell membranes, and make it possible for more drug-loaded nanoparticles entered into the cells to exert their efficacy.[29−35] In addition, it has been found that the binding strength between the polymer nanocarriers and membranes depended on the number density of CP groups, and it can be improved as the increase of the number density of CP groups in a range.[29,31] But with the gain of polymer molecular weight, the entropic exclusion between the polymer chain and potentially binding species out of the cell membranes, like glycocalyx, plays the indispensable role in the interaction between the NDDS and membranes,[29] and this is why the $PMCP_{180}$-s-s-PCL_{90} produces a small increase in cellular uptake efficiency relative to $PMCP_{120}$-s-s-PCL_{90}.

3.4. In Vitro Drug Release Triggered via Glutathione. It is one of the most important issues for the drug-delivery systems to release the loaded-drug effectively after they entered into the tumor cells. To improve the release efficiency of Dox, we integrated the "disulfide bridge" into the polymer chain to conjugate the hydrophobic PCL and water-soluble PMCP. It has been found that the cleavage of "disulfide bridges" can be accelerated when they encounter high glutathione concentration,[10] and the concentration of glutathione in intracellular environment (10 mM) is much higher than that in the extracellular milieu (<10 μM),[41] which made it possible for the disulfide bonds cleaved once these drug-loaded nanoparticles entered into the tumor cells, and then the cargo was released more effectively. In order to confirm the efficiency of bioreducible drug release, in vitro drug release at the milieu with or without 10 mM glutathione and the controlled experiment were determined. It can be found from Figure 5 that only 28.6% Dox was released after the drug-loaded $PMCP_{120}$-s-s-PCL_{90} was incubated at PBS without glutathione for 36 h, but about 61.7% Dox was release effectively after incubated with 10 mM glutathione for same time scale, suggesting the $PMCP_{120}$-s-s-PCL_{90} system was not only stable before they enter into the tumor cells but can also collapse effectively after they entered into the tumor cells. In the controlled experiment, the in vitro release of drug-loaded $PMCP_{85}$-*b*-PCL_{77} exhibited an inefficient release profile under the same conditions compared with the $PMCP_{120}$-s-s-PCL_{90} in imitative intracellular milieu.

3.5. Cellular Proliferation Inhibition. Celltiter-Blue assay was used to evaluate in vitro cytotoxicity of Dox-loaded systems. The MCF-7 cells were incubated with Dox-loaded polymer of $PMCP_{120}$-s-s-PCL_{90}, $PMCP_{85}$-*b*-PCL_{77}, or $PMPC_{150}$-s-s-PCL_{90} for 2 h, and then incubated with fresh DMEM for another 22 h. As expected, compared with the other two controlled systems, the Dox-loaded $PMCP_{120}$-s-s-PCL_{90}

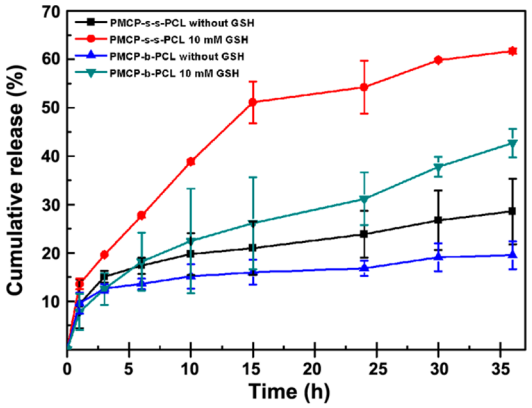

Figure 5. In vitro release curves, Dox released from polymers of $PMCP_{120}$-s-s-PCL_{90}, and $PMCP_{85}$-*b*-PCL_{77} nanoparticles in PBS buffer with or without 10 mM glutathione.

showed enhanced cytotoxicity to the cell lines MCF-7 (Figure 6a), which can be attributed to the enhanced internalization

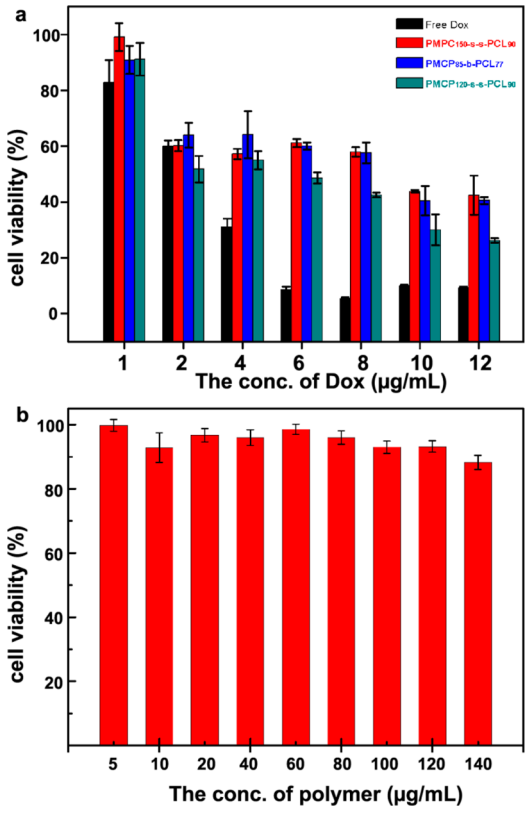

Figure 6. (a) Incubated with different concentrations of free Dox, Dox-loaded $PMCP_{120}$-s-s-PCL_{90}, $PMPC_{150}$-s-s-PCL_{90}, and $PMCP_{85}$-*b*-PCL_{77} for 2 h, then incubated with serum-free DMEM for another 22 h; (b) MCF-7 cells incubated with gradient concentrations of the $PMCP_{120}$-s-s-PCL_{90} for 24 h.

efficiency induced by the PMCP and improved intracellular drug release triggered by the cleavage of bioreducible linkers. Interestingly, the groups $PMCP_{85}$-*b*-PCL_{77} and $PMPC_{150}$-s-s-PCL_{90} exhibit similar therapeutic efficacy, which maybe because that although the former has the advantage to enhance the cellular uptake, the sluggish intracellular drug release contrast to the $PMPC_{150}$-s-s-PCL_{90} causes the Dox cannot effectively diffuse into nucleus to exert their cytostatic effects. The vitro

DOI: 10.1021/acsami.7b03317
ACS Appl. Mater. Interfaces 2017, 9, 15986−15994

cytotoxicity of blank $PMCP_{120}$-s-s-PCL_{90} nanocarrier toward MCF-7 was also estimated using a Celltiter-Blue assay. As shown in Figure 6b, the cell viability assays demonstrated the $PMCP_{120}$-s-s-PCL_{90} has good biocompatibility and low toxicity. The same tendency was found in other two tumor cell lines (Figures S10 and S11). We also chose MCF-7 as the model to study the cytotoxicity of these polymer nanocarriers in the presence of serum (as shown in Figure S12). It was found that these polymer nanocarriers showed similar toxicity with those in the absence of serum. Combined with the previous cellular internalization results, it can be concluded that this CP-based polymer nanocarriers showed increased cellular internalization, low toxicity and good biocompatibility, which are independent of the existence of serum. All these results indicated that the $PMCP_{120}$-s-s-PCL_{90} can be used as a novel delivery system to conquer some stubborn challenges in current tumor treatment.

4. CONCLUSION

In summary, we designed and synthesized a new polymer delivery system, whose specific structures and features can be used to improve the therapy efficacy in tumor treatment. The integration of multivalent CP into the delivery system effectively enhanced the cellular internalization over a short time via the specific and strong interactions between PMCP and cell membrane. Meanwhile, the accelerated cleavage of bioreducible "disulfide bridge" between the hydrophobic PCL and water-soluble PMCP in intracellular milieu improved the Dox escape from the delivery system to cytoplasm to exert their cytostatic effects. Importantly, the in vitro cytotoxicity assays showed that the Dox-loaded $PMCP_{120}$-s-s-PCL_{90} had enhanced cytotoxicity to tumor cells. As a proof of concept, the multivalent CP decorating materials showed great potential to improve the internalization efficiency in drug delivery application.

■ ASSOCIATED CONTENT

Supporting Information

The Supporting Information is available free of charge on the ACS Publications website at DOI: 10.1021/acsami.7b03317.

Synthesis and characterization of the control, additional confocal images, flow cytometry analysis, and cell viability of other cell lines (A549 & HepG2) (PDF)

■ AUTHOR INFORMATION

Corresponding Authors

*E-mail: xjma@ciac.ac.cn.

*E-mail: xfyu@ciac.ac.cn.

ORCID

Xifei Yu: 0000-0003-4654-6941

Notes

The authors declare no competing financial interest.

■ ACKNOWLEDGMENTS

The financial support from the Nation Natural Science Foundation of China (21304096, 21474103, 21603214, 21674109) is acknowledged.

■ REFERENCES

(1) Peer, D.; Karp, J. M.; Hong, S.; FaroKhzad, O. C.; Margalit, R.; Langer, R. Nanocarriers as an Emerging Platform for Cancer Therapy. *Nat. Nanotechnol.* **2007**, *2*, 751−760.

(2) Mura, S.; Nicolas, J.; Couvreur, P. Stimuli-Responsive Nanocarriers for Drug Delivery. *Nat. Mater.* **2013**, *12*, 991−1003.

(3) Chen, W.; Yuan, Y.; Cheng, D.; Chen, J.; Wang, L.; Shuai, X. Co-Delivery of Doxorubicin and siRNA with Reduction and pH Dually Sensitive Nanocarrier for Synergistic Cancer Therapy. *Small* **2014**, *10*, 2678−2687.

(4) Robertson, J. D.; Yealland, G.; Avila-Olias, M.; Chierico, L.; Bandmann, O.; Renshaw, S. A.; Battaglia, G. pH-Sensitive Tubular Polymersomes: Formation and Applications in Cellular Delivery. *ACS Nano* **2014**, *8*, 4650−4661.

(5) Chen, X.; Parelkar, S. S.; Henchey, E.; Schneider, S.; Emrick, T. PolyMPC-Doxorubicin Prodrugs. *Bioconjugate Chem.* **2012**, *23*, 1753−1763.

(6) Wang, H.; Xu, F.; Li, D.; Liu, X.; Jin, Q.; Ji, J. Bioinspired Phospholipid Polymer Prodrug as a pH-Responsive Drug Delivery System for Cancer Therapy. *Polym. Chem.* **2013**, *4*, 2004−2010.

(7) Wang, Y. C.; Wang, F.; Sun, T. M.; Wang, J. Redox-Responsive Nanoparticles from the Single Disulfide Bond-Bridged Block Copolymer as Drug Carriers for Overcoming Multidrug Resistance in Cancer Cells. *Bioconjugate Chem.* **2011**, *22*, 1939−1945.

(8) Zhang, Y.; He, J.; Cao, D.; Zhang, M.; Ni, P. Galactosylated Reduction and pH Dual-responsive Triblock Terpolymer Gal-PEEP-a-PCL-ss-PDMAEMA: a Multifunctional Carrier for the Targeted and Simultaneous Delivery of Doxorubicin and DNA. *Polym. Chem.* **2014**, *5*, 5124−5138.

(9) Kumar, A.; Lale, S. V.; Mahajan, S.; Choudhary, V.; Koul, V. ROP and ATRP Fabricated Dual Targeted Redox Sensitive Polymersomes Based on pPEGMA-PCL-ss-PCL-pPEGMA Triblock Copolymers for Breast Cancer Therapeutics. *ACS Appl. Mater. Interfaces* **2015**, *7*, 9211−9227.

(10) Ahmed, A.; Liu, S.; Pan, Y.; Yuan, S.; He, J.; Hu, Y. Multicomponent Polymeric Nanoparticles Enhancing Intracellular Drug Release in cancer cells. *ACS Appl. Mater. Interfaces* **2014**, *6*, 21316−21324.

(11) Du, J. Z.; Du, X. J.; Mao, C. Q.; Wang, J. Tailor-Made Dual pH-sensitive Polymer-doxorubicin Nanoparticles for Efficient Anticancer Drug Delivery. *J. Am. Chem. Soc.* **2011**, *133*, 17560−17563.

(12) Guo, X.; Shi, C.; Yang, G.; Wang, J.; Cai, Z.; Zhou, S. Dual-Responsive Polymer Micelles for Target-Cell-Specific Anticancer Drug Delivery. *Chem. Mater.* **2014**, *26*, 4405−4418.

(13) Guo, X.; Wei, X.; Jing, Y.; Zhou, S. Size Changeable Nanocarriers with Nuclear Targeting for Effectively Overcoming Multidrug Resistance in Cancer Therapy. *Adv. Mater.* **2015**, *27*, 6450−6456.

(14) Li, J.; Yu, X.; Wang, Y.; Yuan, Y.; Xiao, H.; Cheng, D.; Shuai, X. A Reduction and pH Dual-Sensitive Polymeric Vector for Long-circulating and Tumor-Targeted siRNA Delivery. *Adv. Mater.* **2014**, *26*, 8217−8224.

(15) Huang, M. M.; Zhao, K. J.; Wang, L.; Lin, S. Q.; Li, J. J.; Chen, J. B.; Zhao, C. G.; Ge, Z. S. Dual Stimuli-Responsive Polymer Prodrugs Quantitatively Loaded by Nanoparticles for Enhanced Cellular Internalization and Triggered Drug Release. *ACS Appl. Mater. Interfaces* **2016**, *8*, 11226−11236.

(16) Zhou, Z.; Shen, Y.; Tang, J.; Fan, M.; Van Kirk, E. A.; Murdoch, W. J.; Radosz, M. Charge-Reversal Drug Conjugate for Targeted Cancer Cell Nuclear Drug Delivery. *Adv. Funct. Mater.* **2009**, *19*, 3580−3589.

(17) Wang, S.; Zhang, S.; Liu, J.; Liu, Z.; Su, L.; Wang, H.; Chang, J. pH- and Reduction-Responsive Polymeric Lipid Vesicles for Enhanced Tumor Cellular Internalization and Triggered Drug Release. *ACS Appl. Mater. Interfaces* **2014**, *6*, 10706−10713.

(18) Robertson, J. D.; Yealland, G.; Avila-Olias, M.; Chierico, L.; Bandmann, O.; Renshaw, S. A.; Battaglia, G. pH-Sensitive Tubular Polymersomes: Formation and Applications in Cellular Delivery. *ACS Nano* **2014**, *8*, 4650−4661.

(19) Albanese, A.; Tang, P. S.; Chan, W. C. W. The Effect of Nanoparticle Size, Shape, and Surface Chemistry on Biological Systems. *Annu. Rev. Biomed. Eng.* **2012**, *14*, 1−16.

(20) Chithrani, B. D.; Ghazani, A. A.; Chan, W. C. W. Determining the Size and Shape Dependence of Gold Nanoparticle Uptake into Mammalian Cells. *Nano Lett.* **2006**, *6*, 662−668.
(21) Geng, Y.; Dalhaimer, P.; Cai, S. S.; Tsai, R.; Tewari, M.; Minko, T.; Discher, D. E. Shape Effects of Filaments Versus Spherical Particles in Flow and Drug Delivery. *Nat. Nanotechnol.* **2007**, *2*, 249−255.
(22) Gratton, S. E. A.; Ropp, P. A.; Pohlhaus, P. D.; Luft, J. C.; Madden, V. J.; Napier, M. E.; DeSimone, J. M. The Effect of Particle Design on Cellular Internalization Pathways. *Proc. Natl. Acad. Sci. U. S. A.* **2008**, *105*, 11613−11618.
(23) Copolovici, D. M.; Langel, K.; Eriste, E.; Langel, U. Cell-Penetrating Peptides: Design, Synthesis, and Applications. *ACS Nano* **2014**, *8*, 1972−1994.
(24) Di Pisa, M.; Chassaing, G.; Swiecicki, J. M. Translocation Mechanism(s) of Cell-Penetrating Peptides: Biophysical Studies Using Artificial Membrane Bilayers. *Biochemistry* **2015**, *54*, 194−207.
(25) Hu, X. L.; Liu, S.; Huang, Y. B.; Chen, X. S.; Jing, X. B. Biodegradable Block Copolymer-Doxorubicin Conjugates via Different Linkages: Preparation, Characterization, and In Vitro Evaluation. *Biomacromolecules* **2010**, *11*, 2094−2102.
(26) Amaral, A. J.; Pasparakis, G. Macromolecular Cell Surface Engineering for Accelerated and Reversible Cellular Aggregation. *Chem. Commun.* **2015**, *51*, 17556−17559.
(27) Ellis, G. A.; Palte, M. J.; Raines, R. T. Boronate-Mediated Biologic Delivery. *J. Am. Chem. Soc.* **2012**, *134*, 3631−3634.
(28) Wang, J.; Wu, W.; Zhang, Y. J.; Wang, X.; Qian, H. Q.; Liu, B. R.; Jiang, X. Q. The Combined Effects of Size and Surface Chemistry on the Accumulation of Boronic Acid-Rich Protein Nanoparticles in Tumors. *Biomaterials* **2014**, *35*, 866−878.
(29) Yu, X.; Liu, Z.; Janzen, J.; Chafeeva, I.; Horte, S.; Chen, W.; Kainthan, R. K.; Kizhakkedathu, J. N.; Brooks, D. E. Polyvalent Choline Phosphate as a Universal Biomembrane Adhesive. *Nat. Mater.* **2012**, *11*, 468−476.
(30) Yu, X.; Yang, X.; Horte, S.; Kizhakkedathu, J. N.; Brooks, D. E. ATRP Synthesis of Poly(2-(methacryloyloxy)ethyl choline phosphate): a Multivalent Universal Biomembrane Adhesive. *Chem. Commun.* **2013**, *49*, 6831−6833.
(31) Yu, X.; Zou, Y.; Horte, S.; Janzen, J.; Kizhakkedathu, J. N.; Brooks, D. E. Thermal Reversal of Polyvalent Choline Phosphate, a Multivalent Universal Biomembrane Adhesive. *Biomacromolecules* **2013**, *14*, 2611−2621.
(32) Yu, X.; Yang, X.; Horte, S.; Kizhakkedathu, J. N.; Brooks, D. E. A pH and Thermosensitive Choline Phosphate-Based Delivery Platform Targeted to the Acidic Tumor Microenvironment. *Biomaterials* **2014**, *35*, 278−286.
(33) Yu, X.; Yang, X.; Horte, S.; Kizhakkedathu, J. N.; Brooks, D. E. A Thermoreversible Poly(choline phosphate) Based Universal Biomembrane Adhesive. *Macromol. Biosci.* **2014**, *14*, 334−339.
(34) Yang, X.; Li, N.; Constantinesco, I.; Yu, K.; Kizhakkedathu, J. N.; Brooks, D. E. Choline phosphate functionalized cellulose membrane: A Potential Hemostatic Dressing Based on a Unique Bioadhesion Mechanism. *Acta Biomater.* **2016**, *40*, 212−225.
(35) Wang, W.; Wang, B.; Ma, X.; Liu, S.; Shang, X.; Yu, X. Tailor-Made pH-Responsive Poly(choline phosphate) Prodrug as a Drug Delivery System for Rapid Cellular Internalization. *Biomacromolecules* **2016**, *17*, 2223−2232.
(36) Perttu, E. K.; Kohli, A. G.; Szoka, F. C. Inverse-Phosphocholine Lipids: a Remix of a Common Phospholipid. *J. Am. Chem. Soc.* **2012**, *134*, 4485−4488.
(37) Wang, F.; Liu, J. A Stable Lipid/TiO_2 Interface with Headgroup-Inversed Phosphocholine and a Comparison with SiO_2. *J. Am. Chem. Soc.* **2015**, *137*, 11736−11742.
(38) Hu, G.; Emrick, T. Functional Choline Phosphate Polymers. *J. Am. Chem. Soc.* **2016**, *138*, 1828−1831.
(39) Cunningham, A.; Oh, J. K. New Design of Thiol-Responsive Degradable Polylactide-Based Block Copolymer Micelles. *Macromol. Rapid Commun.* **2013**, *34*, 163−168.
(40) Ding, M.; Li, J.; He, X.; Song, N.; Tan, H.; Zhang, Y.; Zhou, L.; Gu, Q.; Deng, H.; Fu, Q. Molecular Engineered Super-Nanodevices: Smart and Safe Delivery of Potent Drugs into Tumors. *Adv. Mater.* **2012**, *24*, 3639−3645.
(41) Ko, N. R.; Oh, J. K. Glutathione-Triggered Disassembly of Dual Disulfide Located Degradable Nanocarriers of Polylactide-Based Block Copolymers for Rapid Drug Release. *Biomacromolecules* **2014**, *15*, 3180−3189.
(42) Zhao, X.; Liu, P. Reduction-Responsive Core-Shell-Corona Micelles Based on Triblock Copolymers: Novel Synthetic Strategy, Characterization, and Application as a Tumor Microenvironment-Responsive Drug Delivery System. *ACS Appl. Mater. Interfaces* **2015**, *7*, 166−174.
(43) Zhang, Q.; He, J.; Zhang, M.; Ni, P. A Polyphosphoester-Conjugated Camptothecin Prodrug with Disulfide Linkage for Potent Reduction-Triggered Drug Delivery. *J. Mater. Chem. B* **2015**, *3*, 4922−4932.
(44) Ko, N. R.; Yao, K.; Tang, C.; Oh, J. K. Synthesis and Thiol-Responsive Degradation of Polylactide-Based Block Copolymers Having Disulfide Junctions Using ATRP and ROP. *J. Polym. Sci., Part A: Polym. Chem.* **2013**, *51*, 3071−3080.
(45) Liu, J.; Pang, Y.; Huang, W.; Huang, X.; Meng, L.; Zhu, X.; Zhou, Y.; Yan, D. Bioreducible Micelles Self-Assembled from Amphiphilic Hyperbranched Multiarm Copolymer for Glutathione-Mediated Intracellular Drug Delivery. *Biomacromolecules* **2011**, *12*, 1567−1577.
(46) Etrych, T.; Jelinkova, M.; Rihova, B.; Ulbrich, K. New HPMA Copolymers Containing Doxorubicin Bound via pH-Sensitive Linkage: Synthesis and Preliminary in Vitro and in Vivo Biological Properties. *J. Controlled Release* **2001**, *73*, 89−102.
(47) Ulbrich, K.; Subr, V. Polymeric Anticancer Drugs with pH-Controlled Activation. *Adv. Drug Delivery Rev.* **2004**, *56*, 1023−1050.
(48) Liu, J.; Pang, Y.; Huang, W.; Zhu, Z.; Zhu, X.; Zhou, Y.; Yan, D. Redox-Responsive Polyphosphate Nanosized Assemblies: a Smart Drug Delivery Platform for Cancer Therapy. *Biomacromolecules* **2011**, *12*, 2407−2415.
(49) Yang, Q.; Tan, L.; He, C.; Liu, B.; Xu, Y.; Zhu, Z.; Shao, Z.; Gong, B.; Shen, Y. M. Redox-Responsive Micelles Self-Assembled from Dynamic Covalent Block Copolymers for Intracellular Drug Delivery. *Acta Biomater.* **2015**, *17*, 193−200.
(50) Duan, X. P.; Xiao, J. S.; Yin, Q.; Zhang, Z. W.; Yu, H. J.; Mao, S. R.; Li, Y. P. Smart pH-Sensitive and Temporal-Controlled Polymeric Micelles for Effective Combination Therapy of Doxorubicin and Disulfiram. *ACS Nano* **2013**, *7*, 5858−5869.
(51) Regev, R.; Yeheskely-Hayon, D.; Katzir, H.; Eytan, G. D. Transport of Anthracyclines and Mitoxantrone Across Membranes by a Flip-Flop Mechanism. *Biochem. Pharmacol.* **2005**, *70*, 161−169.
(52) Regev, R.; Eytan, G. D. Flip-Flop of Doxorubicin Across Erythrocyte and Lipid Membranes. *Biochem. Pharmacol.* **1997**, *54*, 1151−1158.
(53) Krylova, O. O.; Melik-Nubarov, N. S.; Badun, G. A.; Ksenofontov, A. L.; Menger, F. M.; Yaroslavov, A. A. Pluronic L61 Accelerates Flip-Flop and Transbilayer Doxorubicin Permeation. *Chem. - Eur. J.* **2003**, *9*, 3930−3936.

DOI: 10.1021/acsami.7b03317
ACS Appl. Mater. Interfaces 2017, 9, 15986−15994